Available online at www.sciencedirect.com
SCIENCE DIRECT®
Theoretical Population Biology 65 (2004) 75–88
Theoretical Population Biology
http://www.elsevier.com/locate/ytpbi

Age-structured population growth rates in constant and variable environments: a near equilibrium approach

Sonya Dewi[1] and Peter Chesson*

Ecosystem Dynamics Group, Australian National University, Canberra, Australia

Received 6 May 2003

Abstract

General measures summarizing the shapes of mortality and fecundity schedules are proposed. These measures are derived from moments of probability distributions related to mortality and fecundity schedules. Like moments, these measures form infinite sequences, but the first terms of these sequences are of particular value in approximating the long-term growth rate of an age-structured population that is growing slowly. Higher order terms are needed for approximating faster growing populations. These approximations offer a general nonparametric approach to the study of life-history evolution in both constant and variable environments. These techniques provide simple quantitative representations of the classical findings that, with fixed expected lifetime and net reproductive rate, type I mortality and early peak reproduction increase the absolute magnitude of the population growth rate, while type III mortality and delayed peak reproduction reduce this absolute magnitude.

Keywords: Life history; Survivorship curve; Age-dependent mortality and reproduction; Stochasticity; Projection matrix; Δ-measure

1. Introduction

The study of age-structured population growth has a long history in population biology. The most common formulation in the present day assumes discrete times and ages. Population growth is then modeled using a population projection matrix, which can be built from a life table (Leslie, 1945, 1948; Bernadelli, 1941). Application of such models has been extensive, facilitated by the ease of numerical computation and the well-developed body of theory on nonnegative matrices. Continuous formulations, however, can achieve the same ends (Caswell, 2001; Charlesworth, 1994), but are not as widely used.

Most commonly, population projection matrices are applied with constant mortality and fecundity rates (vital rates), which means that population growth is density independent (or alternatively, the population is at equilibrium), and is not affected by environmental variability. The dominant eigenvalue of the projection matrix is then equal to the finite rate of increase (in essence the long-run growth rate), which also serves as a fitness measure. In the study of life-history evolution, some authors have alternatively proposed using expected lifetime reproduction as a fitness measure. However, this measure requires that the population under study is at equilibrium (Kozlowski, 1993).

With constant vital rates, a population reaches a stable age distribution and grows exponentially. This simply means that the population will become very large, if the growth rate is positive, and will become extinct, if the growth rate is negative. Although such exponential growth would not be expected to be sustained for long in nature, such situations are nevertheless highly important in understanding life-history evolution and also in understanding species coexistence. For example, the ESS approach to density-dependent life-history evolution relies critically on analyzing the long-term growth rates of variant types at low density in competition with other types. The growth of a low-density variant can be appropriately analyzed as independent of its own density. Moreover, of most interest is the boundary in parameter space between population increase and decrease, and so it is useful to

*Corresponding author. Present address: Section of Evolution and Ecology, Division of Biological Sciences, University of California, Davis, 1 Shields Avenue, 3331 Storer Hall, Davis, CA 95616-5270, USA. Fax: +530-752-1449.

E-mail addresses: sdewi@cgiar.org (S. Dewi), plchesson@ucdavis.edu (P. Chesson).

[1]Present address: Center for International Forestry Research, Bogor, Indonesia 16680.

0040-5809/$ - see front matter © 2003 Elsevier Inc. All rights reserved.
doi:10.1016/j.tpb.2003.09.002

have techniques that are valid when population growth rates are low. A similar situation arises in the study of species coexistence. There, the invasibility approach, which in different circumstances is applicable to establishing stochastically bounded coexistence (Chesson and Ellner, 1989; Ellner, 1989) or permanent coexistence (Law and Morton, 1996), also analyzes populations growing from low density. Density-dependent feedback within the population is minor, and again of most interest are boundaries in parameter space separating increasing and decreasing populations.

The vital rates of most organisms have some degree of age structure, i.e. the age-specific mortality and fecundity rates do in fact depend on age. The critical feature of the standard population projection matrix approach is that it allows this age specificity to be taken into account simply and naturally. The challenge, however, is to obtain general information on the effects of such age dependence on population growth. One approach has been to use sensitivity analysis. The effects of changing any particular vital rate by a small amount can then be assessed (Caswell, 1978). Using such approaches, evolution of senescence, optimum age of maturity, benefits of being annual, biennial, or perennial, and other similar questions have been explored (Stearns, 1992; Roff, 1992; Charlesworth, 1994; Oli and Dobson, 2003).

Questions like those above are indicative of the fact that general features of life histories are more likely to be determined genetically and subject to natural selection than the individual vital rates for particular age classes. Ideally, life-history evolution theory should connect such features to a fitness measure. However, in the absence of a quantitative measure to summarize the details of vital rates in different age classes, the theory cannot proceed in this way directly. Nevertheless, in some cases a trait that is subject to strong selection can be specified by a single parameter. Age at maturity is one example. To date multidimensional traits, such as mortality and fecundity schedules, have not been quantified in such a way that the selection pressure on them can be assessed in a general way. Instead, sensitivity analysis is commonly applied to a single vital rate, such as the death rate of a particular age class, and hence does not lead to general conclusions about the mortality schedule.

The question we address is how one investigates general properties of a vital-rate schedule, such as its shape. For example, mortality schedules are often classified into three general shapes (types I–III) depending on whether the plot of the log fraction surviving to a particular age is a straightline against age, or is a concave or convex function of age. One response to the question of the effects of the shape of a vital-rate schedule on population growth is to use macroparameter analysis. In macroparameter analysis, vital-rate schedules are given by parametric formulae and the effects of changing the parameters of these formulae are examined (Caswell, 1982). Here we take a more direct nonparametric approach that therefore does not depend on specifying vital-rate schedules by particular formulae. We ask, given an arbitrary mortality or fecundity schedule, can we find general measures of shape that characterize the effects of shape on population growth? Our results are a set of shape measures (which we call Δ-measures) that are analogous to moments or cumulants of a probability distribution. These measures allow us to characterize the effects of the shapes of a vital-rate schedule on population growth.

The proposed measures are most useful when population growth rate is low, and so it is a near equilibrium approach. However, it is important to keep in mind that in the ESS approach to life-history evolution, and in the invasibility approach to species coexistence, the chief interest is in determining the boundaries of regions of parameter space delineating positive and negative growth, as discussed above. Hence, a near equilibrium approach is perfectly applicable to this goal.

We anticipate that these shape measures of vital-rate schedules will lead to new insights into life-history evolution and into competitive coexistence (Dewi, 1998; Dewi and Chesson, 2003). We show here that they can be used also in situations where the vital rates change with time due to environmental variation. In that case, where projection matrices follow a Markov process, a quadratic approximation to the long-term population growth rate for small variance has been developed (Tuljapurkar, 1982, 1990, 1997). Our vital-rate shape measures are applied to the situation where the total fecundity of the population varies with the environment, but the fecundity schedule retains its shape. Thus, the fecundities of different age classes are assumed to respond proportionately to their common varying environment, a situation that can be argued as a reasonable first approximation to reality.

2. General demographic models

The standard, discrete-time demographic model in a constant environment is written in terms of a Lefkovitch matrix as follows:

$$\mathbf{P}(t+1) = \mathbf{L}\mathbf{P}(t), \tag{1}$$

where $\mathbf{P}$ is a column vector of population density of each class at time t, and

$$\mathbf{L} = \begin{pmatrix} b_1 & b_2 & b_3 & \cdots & b_s \\ (1-\delta_1) & 0 & 0 & \cdots & 0 \\ 0 & (1-\delta_2) & 0 & \cdots & 0 \\ \vdots & \vdots & \ddots & \cdots & \vdots \\ 0 & 0 & \cdots & (1-\delta_{s-1}) & (1-\delta_s) \end{pmatrix}.$$

In this matrix, b_x is the birth rate of an individual in the age range x to $x+1$, and δ_x is the probability of death in one unit of time for an individual in that class.

Note that the above matrix formulation accommodates an infinity of age classes, provided mortality and fecundity do not change after age s, by defining $b_{s+j} = b_s$ and $\delta_{s+j} = \delta_s$ for $j \geqslant 0$. The behavior of this model is well understood, (e.g. Caswell, 2001). Asymptotically in time, each subpopulation (i.e., each age class) grows at exactly the same exponential rate, r, which is the natural log of the dominant eigenvalue of $\mathbf{L}$. The population approaches a stable age distribution, and the proportion of the population in age class x is

$$\frac{e^{-rx}l_x}{\sum_{x=1}^{\infty} e^{-rx}l_x}, \tag{2}$$

where $l_x = \prod_{i=1}^{x-1}(1-\delta_i)$ is the probability that any given individual survives from ages 1 to x.

When the population is stationary ($r = 0$), Eq. (2) reduces to the stationary age distribution

$$\pi_x = \frac{l_x}{\sum_{x=1}^{\infty} l_x}, \tag{3}$$

where $\sum_{x=1}^{\infty} l_x$ is the expected lifetime, and $1/\sum_{x=1}^{\infty} l_x$ is the death rate that corresponds to this expected lifetime in a nonstructured model. We shall refer to this death rate as the "nonstructured" death rate and denote it by $\tilde{\delta}$. With this notation, the stationary age distribution can be written as

$$\pi_x = \tilde{\delta} l_x. \tag{4}$$

For a given mortality schedule, the probability distribution for the age at death of any given individual is

$$\phi_x = \delta_x l_x, \tag{5}$$

which is closely related to the stationary age distribution. Note that both distributions sum to 1, i.e., both are probability distributions.

Defining $P_\cdot(t+1)$ to be the total population size, Eq. (1) implies

$$P_\cdot(t+1) = \sum_{x=1}^{\infty} b_x P_x(t) + \sum_{x=1}^{\infty} (1-\delta_x) P_x(t). \tag{6}$$

If the vital rates are not age-dependent, then $b_x = \tilde{b}$, and $\delta_x = \tilde{\delta}$ for all x, and Eq. (6) is reduced to the simplest population growth equation

$$P_\cdot(t+1) = (1 + \tilde{b} - \tilde{\delta}) P_\cdot(t).$$

3. Structured mortality

First consider structured mortality alone, i.e. assume age-independent reproduction ($b_x = \tilde{b}$ for all x). For age-dependent mortality, we consider the standard classification of survivorship curves due to Pearl and Minner (Roff, 1992). Type I, II and III mortality schedules result, respectively, from increasing δ_x, constant δ_x, and decreasing δ_x with age, x. Hence $\ln l_x$ is, respectively, concave, linear, and convex as a function of x.

With age-independent reproduction, Eq. (6) can be written as

$$P_\cdot(t+1) = \tilde{b} P_\cdot(t) + \sum_{x=1}^{\infty} (1-\delta_x) P_x(t). \tag{7}$$

On attaining a stable age distribution, this equation becomes

$$\begin{aligned} P_\cdot(t+1) &= \tilde{b} P_\cdot(t) + \left(\sum_{x=1}^{\infty} (1-\delta_x) \frac{e^{-rx} l_x}{\sum_{y=1}^{\infty} e^{-ry} l_y} \right) P_\cdot(t) \\ &= (1 + \tilde{b} - \hat{\delta}) P_\cdot(t), \end{aligned} \tag{8}$$

where

$$\begin{aligned} \hat{\delta} &= \frac{\sum_{x=1}^{\infty} \delta_x l_x e^{-rx}}{\sum_{x=1}^{\infty} l_x e^{-rx}} \\ &= \tilde{\delta} \frac{\sum_{x=1}^{\infty} \delta_x l_x e^{-rx}}{\sum_{x=1}^{\infty} \tilde{\delta} l_x e^{-rx}}. \end{aligned} \tag{9}$$

Expression (9) is the average death rate in the population at its stable age distribution, written here as a modification of the age-independent death rate $\tilde{\delta}$, defined above. Note that $\hat{\delta}/\tilde{\delta}$ is a ratio of the Laplace transforms, with argument r, of the age at death distribution and the stationary age distribution. The particular value of r here, of course, is the exponential growth rate of the population,

$$\begin{aligned} r &= \ln\left\{ \frac{P_\cdot(t+1)}{P_\cdot(t)} \right\} \\ &= \ln\{1 + \tilde{b} - \hat{\delta}\}. \end{aligned} \tag{10}$$

Provided each transform exists in a neighborhood with radius greater than r about zero, the standard properties of Laplace transforms imply that

$$\frac{\hat{\delta}}{\tilde{\delta}} = \frac{\sum_{n=0}^{\infty} \frac{(-r)^n}{n!} \mu_n(\delta_x l_x)}{\sum_{n=0}^{\infty} \frac{(-r)^n}{n!} \mu_n(\tilde{\delta} l_x)}, \tag{11}$$

where $\mu_n(p_x) = \sum_{x=1}^{\infty} x^n p_x$ is the nth moment of the probability distribution $\{p_x\}$. It is now just a short step to the shape measures for the mortality schedule that we seek. Using the ratio theorem for power series (Gradshtein and Ryzhik, 1980) shape measures, Δ_m, can be defined as the coefficients in the power series for the ratio of $\hat{\delta}/\tilde{\delta}$, i.e.

$$\hat{\delta} = \tilde{\delta} \sum_{n=0}^{\infty} (-r)^n \Delta_m^{(n)}, \tag{12}$$

where:

$$\Delta_m^{(0)} = 1,$$
$$\Delta_m^{(1)} = \mu_1(\delta_x l_x) - \mu_1(\tilde{\delta} l_x),$$
$$\Delta_m^{(2)} = \frac{1}{2}(\mu_2(\delta_x l_x) - \mu_2(\tilde{\delta} l_x)) - (\mu_1(\delta_x l_x) - \mu_1(\tilde{\delta} l_x))\mu_1(\tilde{\delta} l_x),$$
$$\Delta_m^{(n)} = \frac{\mu_n(\delta_x l_x)}{n!} - \sum_{k=1}^{n} \Delta_m^{(n-k)} \frac{\mu_k(\tilde{\delta} l_x)}{k!} \quad \text{for } n>0.$$

Independent of r, the Δ_m's are characteristics of the mortality schedule. There are two important uses of these characteristics. First, the Δ_m's define shape characteristics for the mortality schedule in terms of the moment differences between the distribution of the age at death and the stationary age distribution. Note that as these two distributions are identical for a type I mortality schedule, these quantities measure deviations from a type I mortality schedule, i.e. they measure deviations from age-independent mortality. Simple piecewise linear examples of types I–III mortality schedules with their $\Delta_m^{(1)}$ are shown in Fig. 1.

A second use of these measures is that they permit understanding of the effects of age structure on population growth through the series expansion (12) for $\hat{\delta}$, which gives the death rate in the population at the stable age-distribution appearing in formula (10) for r. This death rate is not independent of r, but the power series equation for $\hat{\delta}$ enables a first-order approximation to r i.e., with error $o(r)$, by linearizing Eq. (10) in r. Potentially, more accurate higher order approximations to r are also available from polynomial approximations of Eq. (10), but their practical utility seems limited.

In general, the $\Delta_m^{(n)}$ depend on differences of moments, up to order n, of the two distributions. The quantity $\Delta_m^{(1)}$ measures the difference between the mean age at death for any given cohort of individuals and the mean age of a stationary population, and $\Delta_m^{(2)}$ measures half the difference between the variances of the two distributions plus half the square of $\Delta_m^{(1)}$:

$$\Delta_m^{(2)} = \tfrac{1}{2}[\mathrm{var}(\delta_x l_x) - \mathrm{var}(\tilde{\delta} l_x) + (\Delta_m^{(1)})^2]. \tag{13}$$

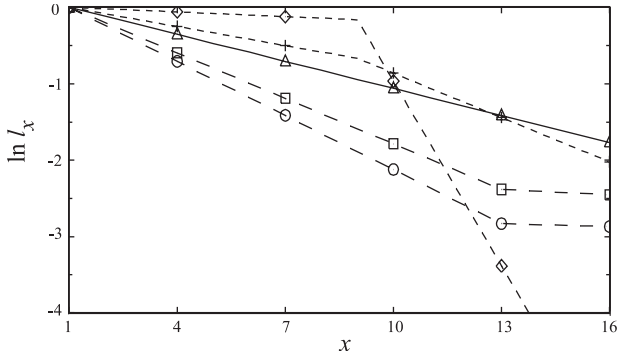

Fig. 1. Mortality schedules of type I (short dashes) with $\Delta_m = 0.2025$ (+), $\Delta_m = 0.4086$ ($\diamond$), of type II ($\Delta_m = 0$) (solid, $\triangle$) and of type III (long dashes) with $\Delta_m = -4.1589$ ($\circ$), $\Delta_m = -1.9485$ ($\square$).

Fig. 2 compares the age at death and stationary age distributions for several different mortality schedules. For a type II mortality schedule (Fig. 2(b)), the two distributions coincide and so the Δ_m's are all zero. For type III mortality schedules (Figs. 2(c) and (d)), the mean cohort age at death is smaller than mean age of a stationary population, which results in negative $\Delta_m^{(1)}$. Moreover, numerical investigation has consistently shown that the variance of cohort age at death is smaller than the variance of the stationary age distribution, plus the square of $\Delta_m^{(1)}$, which results in negative $\Delta_m^{(2)}$. Type I mortality schedules can be generated with a fixed expected lifetime only if $\Delta_m^{(1)}$ and $\Delta_m^{(2)}$ are small, because of the behavior of the two distributions.

A more intuitive understanding can be gained by rewriting the Δ-measures as

$$\Delta_m^{(1)} = \sum_{x=1}^{\infty} x l_x(\delta_x - \tilde{\delta}), \tag{14}$$

$$\Delta_m^{(2)} = \frac{1}{2}\left(\sum_{x=1}^{\infty} x^2 l_x(\delta_x - \tilde{\delta})\right) - \Delta_m^{(1)} \sum_{x=1}^{\infty} x\tilde{\delta} l_x. \tag{15}$$

The first measure sums the age-specific deviations from constant mortality, weighted by xl_x, which means that later age classes are weighted more heavily relative to the probability of surviving to that age. This measure is clearly zero for type II mortality schedules. For type I mortality schedules, with mortality concentrated in the later age classes, the difference between age-specific mortality and constant mortality is positive in the later, more heavily weighted age classes. The second measure exaggerates the difference $(\delta_x - \tilde{\delta})$ by squaring the age (x) in the weights. Numerical study shows that the extra term in the second measure involving the first measure has an opposite effect but the order of magnitude is smaller than the first term, and hence does not change the sign of the second measure. The relationships between the Δ-measures and the three mortality schedules can be summarized as

$$\Delta_m^{(n)} \begin{cases} >0 & \text{for type I mortality schedule,} \\ =0 & \text{for type II mortality schedule,} \\ <0 & \text{for type III mortality schedule,} \end{cases} \tag{16}$$

for $n = 1, 2$.

We will now use the $\Delta_m^{(1)}$ measure to find an approximation for r in the presence of structured mortality. By truncating series (12) for the average death rate at the second term, we obtain

$$\hat{\delta} = \tilde{\delta}(1 - r\Delta_m^{(1)}) + o(r). \tag{17}$$

Substituting for $\hat{\delta}$ in Eq. (10) we get

$$r = \ln\{1 + \tilde{b} - \tilde{\delta} + \tilde{\delta}\Delta_m^{(1)} r\} + o(r), \tag{18}$$

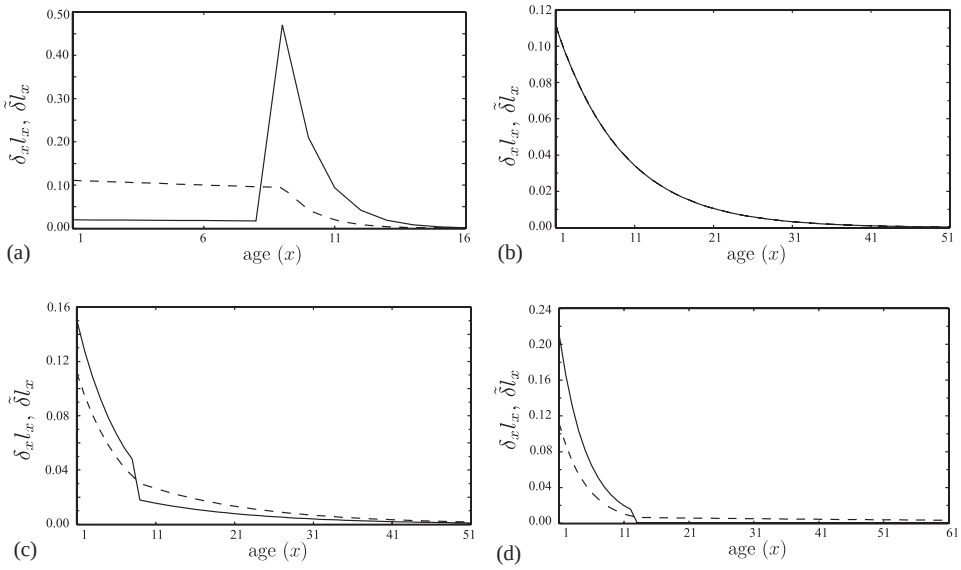

Fig. 2. The distribution of cohort age at death, $\delta_x l_x$, (solid) and of stationary age, $\tilde{\delta} l_x$ (dashes) for a type I mortality schedule with $\Delta_m = 0.409$ (a), a type II mortality schedule (b), a type III mortality schedule with $\Delta_m = -0.410$, (c) and a type III mortality schedule with $\Delta_m = -4.1587$ (d), for expected lifetime = 9.

which rearranges to

$$r = \ln\{1 + \tilde{b} - \tilde{\delta}\} + \ln\left\{1 + \frac{\tilde{\delta}\Delta_m^{(1)} r}{1 + \tilde{b} - \tilde{\delta}}\right\} + o(r)$$
$$= \ln\{1 + \tilde{b} - \tilde{\delta}\} + \frac{\tilde{\delta}\Delta_m^{(1)}}{1 + \tilde{b} - \tilde{\delta}} r + o(r)$$
$$= \tilde{r} + \frac{\tilde{\delta}\Delta_m^{(1)}}{1 + \tilde{b} - \tilde{\delta}} r + o(r), \quad (19)$$

where

$$\tilde{r} = \ln\{1 + \tilde{b} - \tilde{\delta}\},$$

i.e., the value of r that occurs with a type II mortality schedule. Solving Eq. (19) for r now yields

$$r = \frac{\tilde{r}}{1 - \tilde{\delta}\Delta_m^{(1)}/(1 + \tilde{b} - \tilde{\delta})} + o(r). \quad (20)$$

In this study, for simplicity, we illustrate these formulae with just two levels of the death rate, distinguishing early mortality (up to some age s), and later mortality (after age s):

$$\delta_x = \begin{cases} \delta_1 & \text{for } x \leqslant s, \\ [(1-\delta_1)^{s-1}\delta_1]/[\delta_1/\tilde{\delta} - 1 + (1-\delta_1)^s] & \text{for } x > s. \end{cases} \quad (21)$$

With fixed expected lifetime $(1/\tilde{\delta})$, formula (21) has two free parameters, the early death rate, δ_1, and the last age having the early death rate, s. By varying these parameters, types I–III mortality schedules can be generated with a common expected lifetime. The procedure for the graphs below was to vary these two parameters over a rectangular grid of values. The measure $\Delta_m^{(1)}$ for each mortality schedule was calculated from Eq. (14). This procedure generates a range of $\Delta_m^{(1)}$ values, and it is possible to find different mortality schedules with similar $\Delta_m^{(1)}$ and different $\Delta_m^{(2)}$. However, here we will only consider $\Delta_m^{(1)}$ because only it appears in the approximation for r. In the graphs below of r against $\Delta_m^{(1)}$ there is scatter attributable to different values of $\Delta_m^{(2)}$ at fixed $\Delta_m^{(1)}$. In this study, the expected lifetime is held constant so that comparisons between mortality schedules focus on the distribution of mortality over age classes rather than the magnitude of mortality, which is captured by the expected lifetime.

Figs. 3 and 4 show the relationship between $\Delta_m^{(1)}$ and the population growth rate for several values of the birth rate. The population growth rate, calculated as the natural log of the dominant eigenvalue of the matrix $\mathbf{L}$ is compared with that calculated by the first-order approximation to r, Eq. (20).

The quantity $\Delta_m^{(1)}$ does a good job of mapping each mortality schedule into the population growth rate (r) when r is small. From this mapping (Eq. (20)) it can be seen that, with fixed $\tilde{\delta}$ and $\tilde{b}$, $|r|$ is lower with a type III mortality schedule (larger early mortality), and higher with a type I mortality schedule (smaller early mortality). In other words, when the population is increasing, a type I mortality schedule allows faster population growth than other mortality schedules, and when the population is decreasing, a type III mortality schedule results in slower population declines than other mortality schedules. Also, Figs. 3 and 4 show that the effect of age-dependent mortality on population growth rate is greater with greater $\tilde{\delta}$ (shorter lifespan). Therefore, for a population of long-lived organisms, the effect of structured mortality on population growth should only

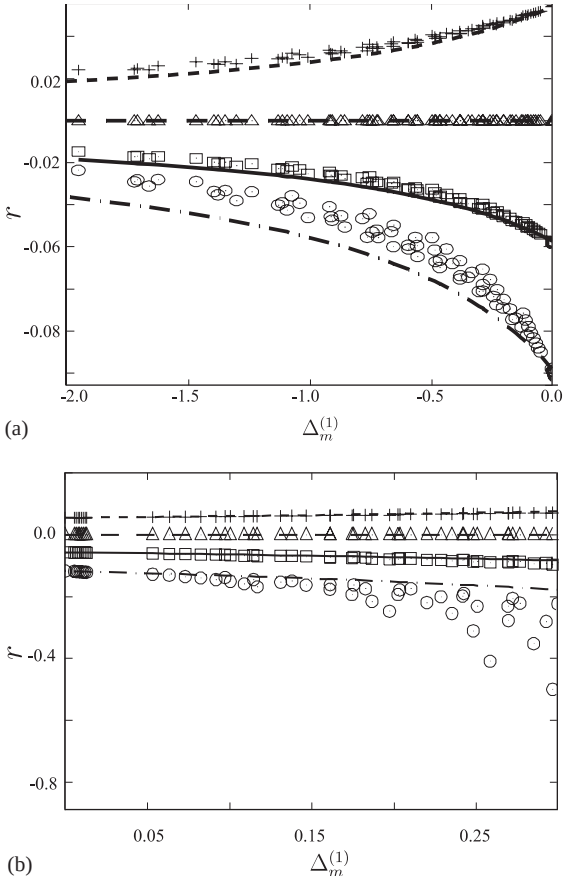

Fig. 3. Population growth rate (r) with mortality schedules of type III (a) and type I (b) with expected lifetime = 9, calculated as ln of the dominant eigenvalue of the projection matrix (symbols), and calculated from the first-order approximation, Eq. (20) (lines). $\tilde{b}$ equals 0 (◦, dashes and dots), 0.0556 (□, solid), 0.1111 (△, dashes) and 0.1667 (+, short dashes).

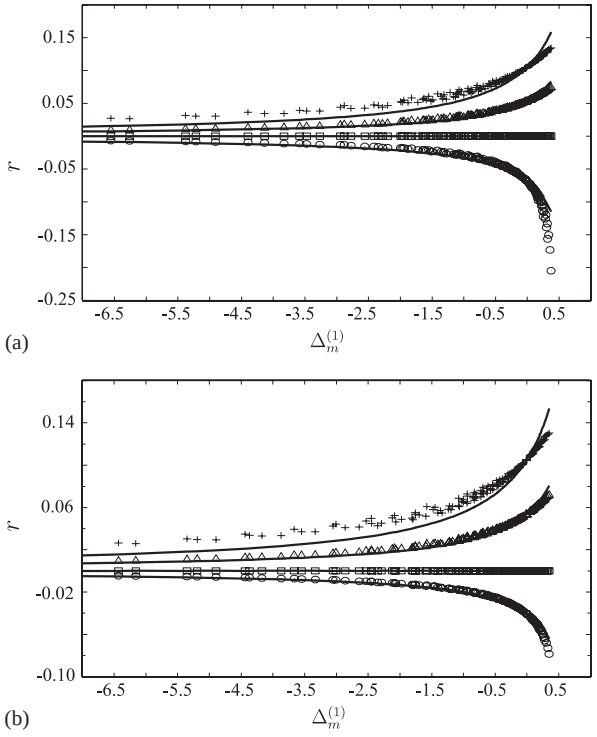

Fig. 4. Population growth rate (r) with mortality schedules of expected lifetime = 15 (a) and expected lifetime = 25 (b), calculated as ln of the dominant eigenvalue of the projection matrix (symbols), and calculated from the first-order approximation, Eq. (20) (lines). $\tilde{b}$ equals 0 (◦), 0.0667 (□), 0.1222 (△) and 0.1778 (+).

be evident when $\Delta_m^{(1)}$ is moderately large, i.e., when there is substantial deviation from a type II mortality schedule.

Eq. (20) gives a simple, functional relationship between the age-independent characteristics ($\tilde{b}$, $\tilde{\delta}$, and $\tilde{r} = \ln(1 + \tilde{b} - \tilde{\delta})$) with mortality schedules and the population growth rate. The population growth rate is expressed in terms of the population growth rate corresponding to a type II mortality schedule ($\tilde{r}$), age-independent death rates ($\tilde{\delta}$), and age-independent birth rates ($\tilde{b}$), and the discrepancy between the actual mortality schedule and a type II mortality schedule (Δ_m). Thus the Δ-measure not only summarizes age-dependent characteristics, but also provides a simple way of assessing the effect of the mortality structure on population growth. Note that fixing $\tilde{b}$ and $\tilde{\delta}$ also fixes the net reproductive rate, R_0, which is equal to $\tilde{b}/\tilde{\delta}$. Thus, R_0 and $\tilde{\delta}$ are an alternative parameter set useful in life-history theory, which allows us to see the effects on population growth of various trade-offs within the constraints of fixed values of these parameters.

4. Structured fecundity

In this section, we will consider a standard demographic model with structured fecundity. The fecundity schedule is expressed in terms of an overall fecundity level, $\tilde{b}$, which is an age-independent parameter, and age-dependent modulation of reproduction of age class x (k_x). The birth rate of age class thus x is $k_x\tilde{b}$.

We will first consider a model without structured mortality, i.e., $\delta_x = \tilde{\delta}$ for all x. We follow the idealized fecundity schedules given by Roff (1992). The particular examples we consider are piecewise linear (Fig. 6) and specified in terms of k_x as follows:

- *Age-independent reproduction*: $k_x = 1$ for all x.
- *Uniform fecundity after maturity*: A juvenile period, with zero fecundity, followed by constant fecundity: $k_x = 0$ for $x < m$, and $k_x = k_m$ for $x \geqslant m$, where m is the age of maturity.
- *Asymptotic fecundity*: k_x increases from the age of maturity until it reaches a maximum value which it sustains for all later ages.
- *Triangular fecundity*: Similar to asymptotic fecundity but after reaching the maximum, fecundity declines until a particular age and then remains constant. Semelparity is a special case of the triangular

schedule in which fecundity peaks at the age of maturity and is zero in all subsequent age-classes.

Without loss of generality the fecundity function, k_x, can be constrained so that $k_x\tilde{\delta}l_x$ sums to one making $k_x\tilde{\delta}l_x$ a probability distribution. This is equivalent to requiring that $\sum_{x=1}^{\infty} k_x l_x = \sum_{x=1}^{\infty} l_x$, which has the effect of fixing $R_0 = \tilde{b}/\tilde{\delta}$.

With age-dependent fecundity specified in this way, Eq. (6) can be written as

$$P_\cdot(t+1) = \tilde{b}\sum_{x=1}^{\infty} k_x P_x(t) + (1-\tilde{\delta})P_\cdot(t). \tag{22}$$

Assuming a stable age distribution, this equation becomes

$$\begin{aligned} P_\cdot(t+1) &= \tilde{b}\left(\frac{\sum_{x=1}^{\infty} k_x e^{-rx} l_x}{\sum_{x=1}^{\infty} e^{-rx} l_x}\right) P_\cdot(t) + (1-\tilde{\delta})P_\cdot(t) \\ &= (1+\hat{b}-\tilde{\delta})P_\cdot(t), \end{aligned} \tag{23}$$

where

$$\hat{b} = \tilde{b}\frac{\sum_{x=1}^{\infty}\tilde{\delta}l_x k_x e^{-rx}}{\sum_{x=1}^{\infty}\tilde{\delta}l_x e^{-rx}}.$$

The term $\hat{b}$ is the average birth rate for all individuals in the population.

Here, the population growth rate is simply

$$r = \ln\{1+\hat{b}-\tilde{\delta}\}. \tag{24}$$

By applying the same techniques used in the previous section, the average birth rate $(\hat{b})$ can be written

$$\hat{b} = \tilde{b}\sum_{n=0}^{\infty}(-r)^n \Delta_f^{(n)}, \tag{25}$$

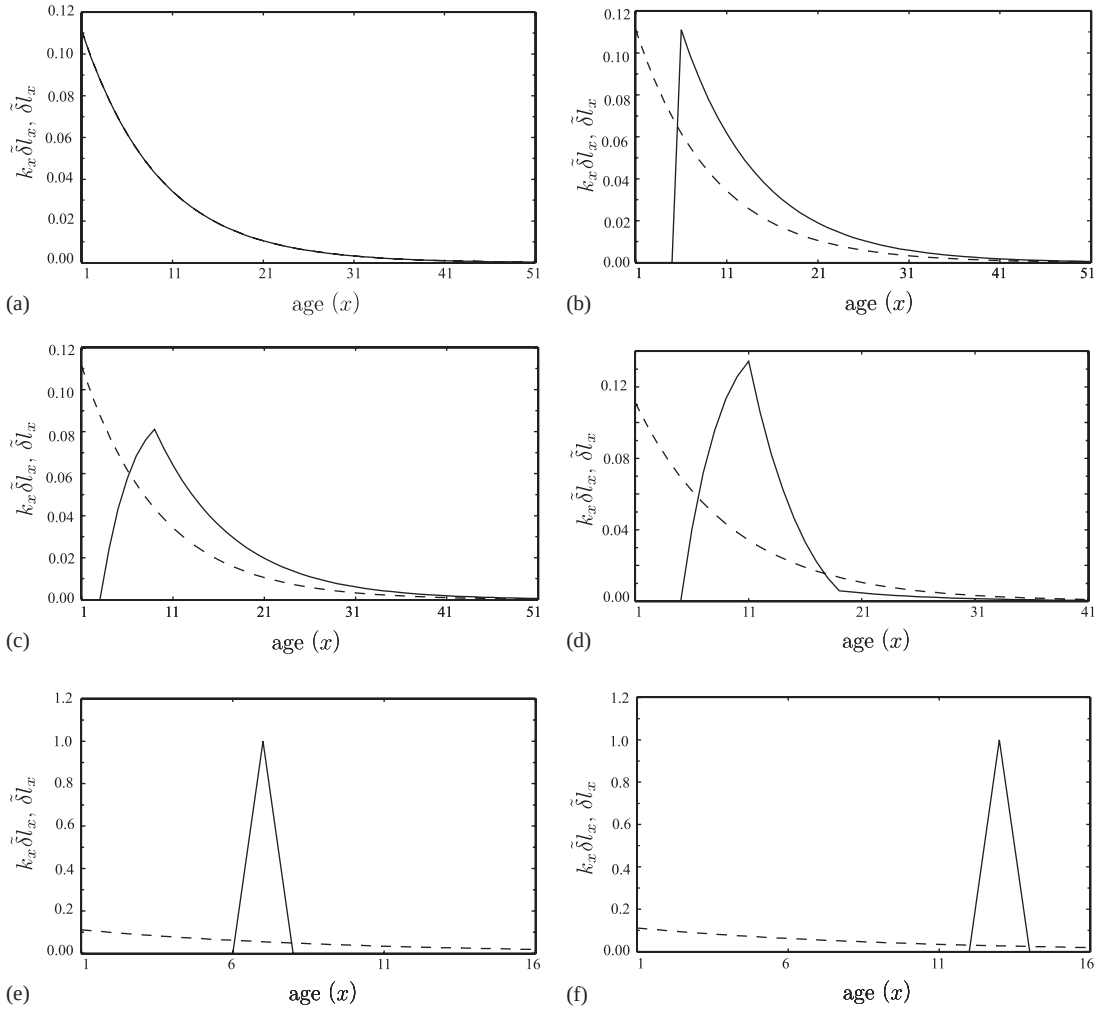

Fig. 5. The distribution of cohort age at reproduction $(k_x\tilde{\delta}l_x)$ (solid), and of stationary age $(\tilde{\delta}l_x)$ (dashes) for age-independent reproduction (a), uniform curve with $\Delta_f = 5$ (b), asymptotic curve with $\Delta_f = 5.1594$ (c), triangular curve with $\Delta_f = 2.7455$ (d), semelparity with age at maturity of 7 with $\Delta_f = -2$ (e), and semelparity with age at maturity of 13 with $\Delta_f = 4$ (f), all with age-independent mortality and expected lifetime = 9.

where

$$\Delta_f^{(0)} = 1,$$
$$\Delta_f^{(1)} = \mu_1(\tilde{\delta} l_x k_x) - \mu_1(\tilde{\delta} l_x),$$
$$\Delta_f^{(2)} = \tfrac{1}{2}(\mu_2(\tilde{\delta} l_x k_x) - \mu_2(\tilde{\delta} l_x)) - [\mu_1(\tilde{\delta} l_x k_x) - \mu_1(\tilde{\delta} l_x)]\mu_1(\tilde{\delta} l_x),$$
$$\Delta_f^{(n)} = \frac{\mu_n(\tilde{\delta} l_x k_x)}{n!} - \sum_{k=1}^{n} \Delta_f^{(n-k)} \frac{\mu_k(\tilde{\delta} l_x)}{k!} \quad \text{for } n > 0.$$

In this case, the two distributions that define the Δ measures are the cohort age at reproduction ($\tilde{\delta} l_x k_x$), and the stationary age distribution ($\tilde{\delta} l_x$) (Fig. 5). Thus Δ_f quantifies the deviation of a fecundity schedule from age-independent reproduction. The first measure ($\Delta_f^{(1)}$) is the difference between mean age at reproduction and the mean age in a stationary population. The second measure ($\Delta_f^{(2)}$) is half the difference between the variances of the two distributions, plus half the square of the first measure:

$$\Delta_f^{(2)} = \tfrac{1}{2}[\mathrm{var}(\tilde{\delta} l_x k_x) - \mathrm{var}(\tilde{\delta} l_x) + (\Delta_f^{(1)})^2]. \tag{26}$$

Fecundity schedules can be classified by the sign of $\Delta_f^{(1)}$ into three forms with the following meanings: (i) Early peak reproduction: the majority of offspring are produced early in life ($\Delta_f^{(1)} < 0$). (ii) Age-independent reproduction when reproduction is spread out evenly throughout the lifespan of an organism ($\Delta_f^{(1)} = 0$). (iii) Delayed peak reproduction when the majority of offspring are produced late in life (i.e., $\Delta_f^{(1)} > 0$). However, this classification is crude, and fails to capture the four types present above (Fig. 6).

A more intuitive understanding of the measures is gained by rewriting Δ_f as

$$\Delta_f^{(1)} = \sum_{x=1}^{\infty} x \tilde{\delta} l_x (k_x - 1), \tag{27}$$

$$\Delta_f^{(2)} = \tfrac{1}{2}\left(\sum_{x=1}^{\infty} x^2 \tilde{\delta} l_x (k_x - 1)\right) - \Delta_f^{(1)} \sum_{x=1}^{\infty} x \tilde{\delta} l_x. \tag{28}$$

The first measure ($\Delta_f^{(1)}$) expresses the difference between each age-dependent modulation of reproduction and constant reproduction (i.e., $k_x = 1$ for all age classes), weighted according to age class, such that more weight is applied to later age classes relative to the probability of surviving to those age classes. The second measure ($\Delta_f^{(2)}$) exaggerates the difference by squaring the age in the weights. The extra term involving the first measure has an opposite effect to the first term, but is smaller and has not changed the sign in numerical studies. The general pattern is:

$$\Delta_f^{(n)} \begin{cases} > 0 & \text{for delayed peak reproduction,} \\ = 0 & \text{for age-independent reproduction,} \\ < 0 & \text{for early peak reproduction,} \end{cases} \tag{29}$$

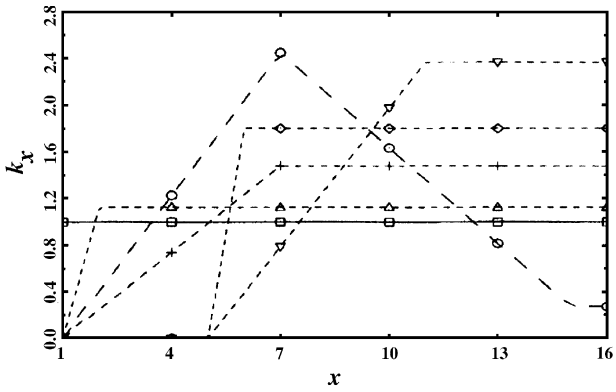

Fig. 6. Age-dependent modulation of reproduction (k_x) for early peak reproduction (long dashes) with $\Delta_f = -1.2545$ ($\circ$), age-independent reproduction ($\square$), and delayed peak reproduction (dashes) with $\Delta_f = 1$ ($\triangle$), $\Delta_f = 3.1594$ ($+$), $\Delta_f = 5$ ($\diamond$), and $\Delta_f = 7.1594$ ($\triangledown$), when combined with a type II mortality schedule.

for $n = 1, 2$. Expressions (27) and (28) provide us with a quantitative classification of fecundity schedules. Fig. 6 shows relationships between $\Delta_f^{(1)}$ and fecundity schedules.

As in the previous section, only $\Delta_f^{(1)}$ will be used to consider the effect of age-dependent fecundity on population growth. The average birth rate satisfies the first-order approximation

$$\hat{b} = \tilde{b}(1 - r\Delta_f^{(1)}) + o(r). \tag{30}$$

Substituting in Eq. (24) we get

$$r = \ln\{1 + \tilde{b} - \tilde{b}\Delta_f^{(1)} r - \tilde{\delta}\} + o(r). \tag{31}$$

Solving Eq. (31), by taking the first-order Taylor approximation of r in the neighborhood of $r = 0$, we get

$$r = \ln\{1 + \tilde{b} - \tilde{\delta}\} - \frac{\tilde{b}\Delta_f^{(1)}}{1 + \tilde{b} - \tilde{\delta}} r + o(r),$$

which rearranges to

$$r = \frac{\tilde{r}}{1 + (\tilde{b}\Delta_f^{(1)})/(1 + \tilde{b} - \tilde{\delta})} + o(r). \tag{32}$$

Eq. (32) gives the functional relationship between fecundity schedules, age-independent vital rates and the population growth rate. Note that the effect of age-dependent fecundity increases with an increase in $\tilde{b}$.

Figs. 7 and 8 show that the general pattern can be captured by $\Delta_f^{(1)}$. The first-order approximation gives good numerical accuracy when r is moderate, and fair accuracy when r is large. The first-order approximation is less accurate with early peak reproduction compared with delayed peak reproduction for r of a similar magnitude. Thus, early peak reproduction, which is mostly produced by triangular curves, is not captured adequately by the first-order Δ-measure alone. In contrast, the effects of other fecundity schedules are

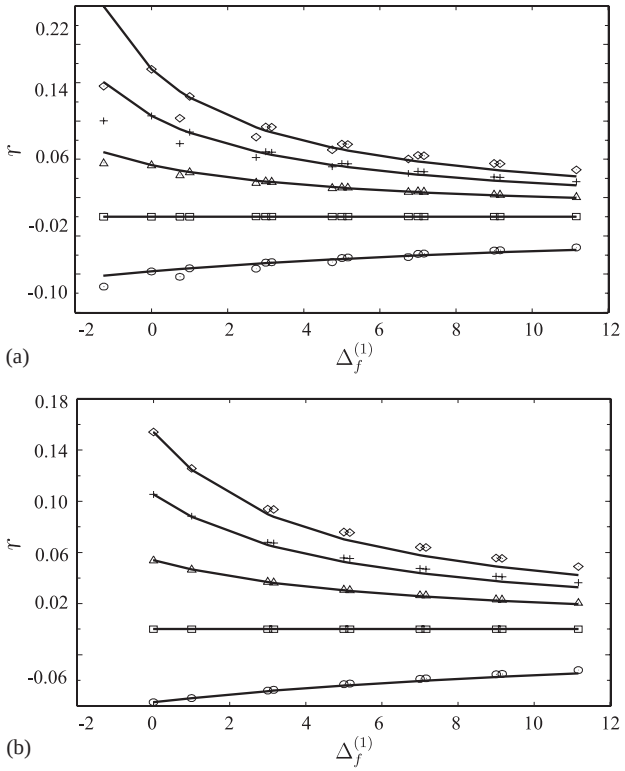

Fig. 7. Population growth rate (r) with age-independent mortality and expected lifetime = 9, for all fecundity schedules (a), and for fecundity schedules other than triangular curves (b), calculated as ln of dominant eigenvalues of the projection matrices (symbols), and calculated from the first-order approximation in Eq. (32) (lines). $\tilde{b}$ equals 0.0556 ($\circ$), 0.1111 ($\square$), 0.1667 ($\triangle$), 0.2222 ($+$) and 0.2778 ($\diamond$).

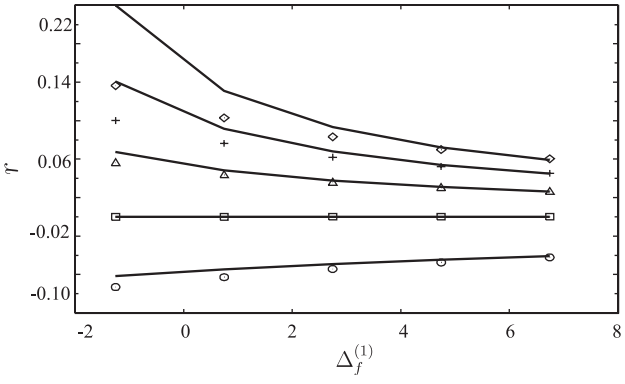

Fig. 8. Population growth rate (r) with age-independent mortality of and expected lifetime = 9 with triangular curves, calculated as ln of dominant eigenvalues of the projection matrices (symbols), and calculated from the first-order approximation in Eq. (32) (lines). $\tilde{b}$ equals 0.0556 ($\circ$), 0.1111 ($\square$), 0.1667 ($\triangle$), 0.2222 ($+$) and 0.2778 ($\diamond$).

captured very with just the first Δ-measure. This is not unexpected as effects of triangular reproductive functions are sensitive to their width, and it is easy to produce different triangular schedules with similar $\Delta_f^{(1)}$'s but different $\Delta_f^{(2)}$'s.

Delayed peak reproduction always gives smaller $|r|$ than early peak reproduction. When a population is increasing, delayed peak reproduction gives lower r, and early peak reproduction gives higher r. The opposite pattern occurs in a decreasing population. This pattern is widely recognized and, shown to be robust in different settings. However, the overall quantitative pattern has not been determined before.

5. Structured mortality and fecundity

We now combine structured mortality and fecundity in the same demographic model. We retain the constraint $\sum_{x=1}^{\infty} k_x l_x = \sum_{x=1}^{\infty} l_x = 1/\tilde{\delta}$ on the k_x values. Fig. 11 shows different fecundity schedules after applying this constraint with types I and III mortality schedules.

With a stable age distribution, the exact value of r is here given by

$$r = \ln\{1 + \hat{b} - \hat{\delta}\}, \tag{33}$$

where $\hat{b}$ and $\hat{\delta}$ are defined as they were in the previous two subsections. Applying the same approximation procedures as used above, we obtain

$$r \approx \frac{\tilde{r}}{1 + (\tilde{b}\Delta_f^{(1)} - \tilde{\delta}\Delta_m^{(1)})/(1 + \tilde{b} - \tilde{\delta})}. \tag{34}$$

Age-dependent fecundity and age-dependent mortality together produce more complex results than either alone. The effects of the mortality and fecundity schedules on the population growth rate are expressed using shape measures scaled by the magnitude of age-independent birth rate ($\tilde{b}$) and death rate ($\tilde{\delta}$). Figs. 9 and 10 show the three distributions: (i) stationary age, (ii) cohort age at death, and (iii) cohort age at reproduction.

Eq. (34) shows that the previous separate findings for the effects of structured mortality and fecundity on population growth continue to apply in combination. In particular, a type III mortality schedule combined with delayed peak reproduction increases r over the unstructured case in decreasing populations, and a type I mortality schedule with the early peak reproduction increases r over the unstructured case in increasing populations, see Fig. 1. These findings are consistent with common belief.

6. Stochastic demographic models

We will now consider the same demographic model as 1, but with temporal fluctuations in birth rates. The matrix model now takes the form

$$\mathbf{P}(t+1) = \mathbf{L}(t)\mathbf{P}(t), \tag{35}$$

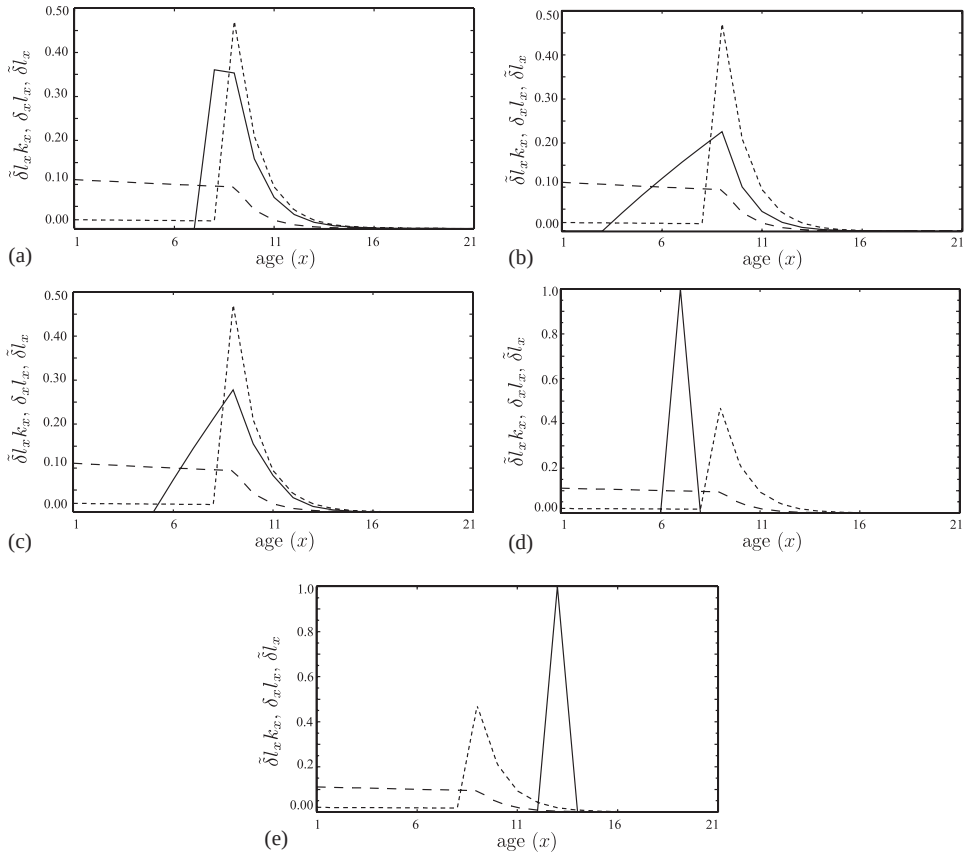

Fig. 9. The distribution of cohort age at reproduction ($\tilde{\delta}l_x k_x$) (solid), cohort age at death ($\delta_x l_x$) (dashes), and stationary age ($\tilde{\delta}l_x$) (short dashes), for a uniform curve with $\Delta_f = 3.3836$ (a), an asymptotic curve with $\Delta_f = 2.6108$ (b), a triangular curve with $\Delta_f = 3.4733$ (c), semelparity with age at maturity of 7 and $\Delta_f = 1.6807$ (d), and semelparity with age at maturity of 13 and $\Delta_f = 7.6807$ (e), all with a type I mortality schedule with $\Delta_m = 0.4086$ and expected lifetime = 9.

where the constant matrix $\mathbf{L}$ of vital rates of Section 2 is replaced by a time-dependent matrix $\mathbf{L}(t)$. The only difference between these two matrices is that b_x is replaced by $\tilde{b}(t)k_x$ in $\mathbf{L}(t)$, with $\tilde{b}(t)$ varying over time to describe temporal variation in fecundity. Eq. (6) becomes

$$\begin{aligned} P_\cdot(t+1) &= \tilde{b}(t)\sum_{x=1}^{\infty} k_x P_x(t) + \sum_{x=1}^{\infty}(1-\delta_x)P_x(t) \\ &= \left(\tilde{b}(t)\sum_{x=1}^{\infty} k_x \frac{P_x(t)}{P_\cdot(t)} + \sum_{x=1}^{\infty}(1-\delta_x)\frac{P_x(t)}{P_\cdot(t)}\right)P_\cdot(t) \\ &= \left(1+\tilde{b}(t)\sum_{x=1}^{\infty} k_x u_x(t) - \sum_{x=1}^{\infty}\delta_x u_x(t)\right)P_\cdot(t) \\ &= (1+\hat{b}(t)-\hat{\delta}(t))P_\cdot(t), \end{aligned} \tag{36}$$

where

$$\hat{\delta}(t) = \sum_{x=1}^{\infty}\delta_x u_x(t),$$

$$\hat{b}(t) = \tilde{b}(t)\sum_{x=1}^{\infty} k_x u_x(t),$$

and $\{u_x(t)\}$ is the actual age distribution at time t. Stochastic ergodicity theory (Lopez, 1961; Cohen, 1977) implies that $\{u_x(t)\}$ should converge in distribution and that, for large t, the quantity ($\bar{r}$) defined as

$$\bar{r} = E\ln\left\{\frac{P_\cdot(t+1)}{P_\cdot(t)}\right\} \tag{37}$$

should approach a constant equal with probability 1 to the actual long-term growth rate of the population. By substituting Eq. (36) into Eq. (37), we obtain

$$\bar{r} = E\ln\{1+\hat{b}(t)-\hat{\delta}(t)\}. \tag{38}$$

In order to proceed simply to an approximation for the long-term growth rate, we shall make the assumption that the species in question is long lived so that the population consists of many cohorts of different ages. With no autocorrelation in birth rate fluctuations over time, these cohorts will be approximately statistically independent. Provided the vital rates of the population do not change sharply with age, which would be at odds with high longevity, it should be possible to replace the actual stochastically fluctuating age distribution in definitions of $\hat{b}(t)$ and $\hat{\delta}(t)$ with the stable age

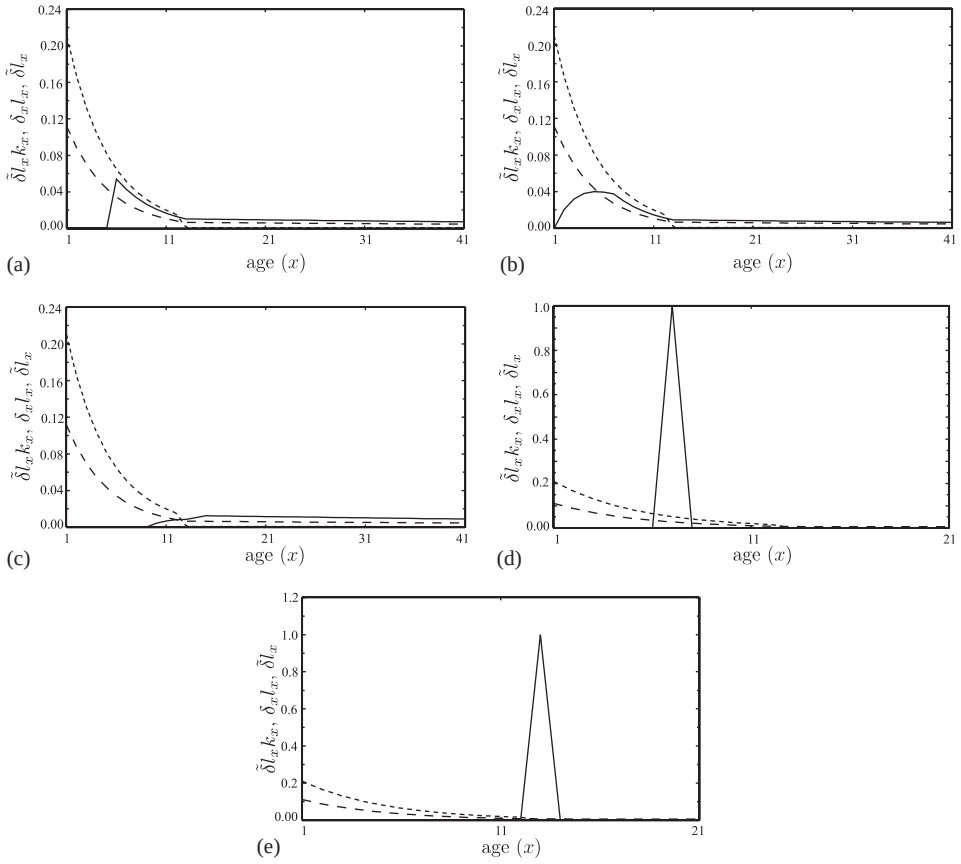

Fig. 10. The distribution of cohort age at reproduction ($\tilde{\delta} l_x k_x$) (solid), cohort age at death ($\delta_x l_x$) (short dashes), and stationary age ($\tilde{\delta} l_x$) (dashes), for a uniform curve with $\Delta_f = 25.3683$ (a), an asymptotic curve with $\Delta_f = 17.0295$ (b), a triangular curve with $\Delta_f = 41.0359$ (c), semelparity with age at maturity of 7 and $\Delta_f = -39.4277$ (d), and semelparity with age at maturity of 13 and $\Delta_f = -33.4277$ (e), all with a type III mortality schedule with $\Delta_m = -4.1589$ and expected lifetime = 9.

distribution attained with constant exponential population growth at a rate $\bar{r}$. In other words, we assume that fluctuations in the age distribution are unimportant, though age structure itself, and fluctuations in birth rates, are both are important in determining the long-term growth rate. Although at first sight, this might seem to seriously limit the application of the results here, numerical results given below suggest that no large errors are thereby introduced.

With this assumption, we can use Δ_m and Δ_f from the previous sections to replace $\hat{\delta}$ and $\hat{k}$ in Eq. (38), to get the average population growth rate as follows:

$$\begin{aligned}\bar{r} &= E\ln[1+\tilde{b}(t)(1-\bar{r}\Delta_f^{(1)}) - \tilde{\delta}(1-\bar{r}\Delta_m^{(1)})] + o(\bar{r}) \\ &= E\ln[1+\tilde{b}(t) - \tilde{\delta} - \bar{r}(\tilde{b}(t)\Delta_f^{(1)} - \tilde{\delta}\Delta_m^{(1)})] + o(\bar{r}). \qquad (39)\end{aligned}$$

The first-order Taylor expansion of expression (39) about $\bar{r} = 0$ is

$$\bar{r} = E\ln[1+\tilde{b}(t) - \tilde{\delta}] - E\left[\frac{\tilde{b}(t)\Delta_f^{(1)} - \tilde{\delta}\Delta_m^{(1)}}{1+\tilde{b}(t)-\tilde{\delta}}\right]\bar{r} + o(\bar{r}). \qquad (40)$$

Solving expression (40) for $\bar{r}$ yields

$$\bar{r} = \frac{E\ln[1+\tilde{b}(t)-\tilde{\delta}]}{1+E[\tilde{b}(t)/(1+\tilde{b}(t)-\tilde{\delta})]\Delta_f^{(1)} - E[1/(1+\tilde{b}(t)-\tilde{\delta})]\tilde{\delta}\Delta_m^{(1)}}.$$

This formula will normally require numerical integration using the distribution of $\tilde{b}(t)k_i$ for evaluation. Alternatively, making some assumptions about the magnitude of the stochastic variation permits closed-form calculation, as follows.

Let b^* be the geometric mean of $\tilde{b}(t)$, i.e. $e^{E\ln\tilde{b}(t)}$, and let $\sigma^2 = \mathrm{var}[\ln\tilde{b}(t)]$. We assume that $\mu = E[\ln\tilde{b}(t) - \ln\tilde{\delta}] = O(\sigma^2)$. With this assumption, Eq. (40) implies that $\bar{r} = O(\sigma^2)$. Removing terms of smaller order from Eq. (39), we obtain

$$\bar{r} = E\ln\left[1+\tilde{\delta}\left(\frac{b^*}{\tilde{\delta}}e^X - 1\right)\right] - \frac{b^*\Delta_f^{(1)} - \tilde{\delta}\Delta_m^{(1)}}{1+b^*-\tilde{\delta}}\bar{r}, \qquad (41)$$

where

$$X = \ln\left\{\frac{\tilde{b}(t)}{b^*}\right\}.$$

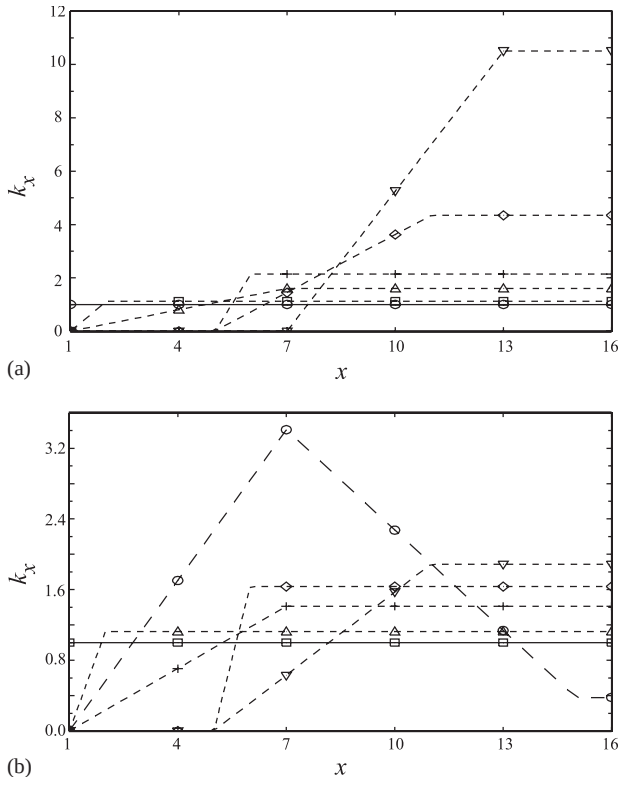

Fig. 11. A type I mortality schedule with $\Delta_m = 0.4086$, with age-independent reproduction ($\circ$), and delayed peak reproduction, with $\Delta_f = 0.5399$ ($\square$), $\Delta_f = 1.6264$ ($\triangle$), $\Delta_f = 2.7015$ ($+$), $\Delta_f = 3.5373$ ($\diamond$), and $\Delta_f = 4.5645$ (∇)(a). A type III mortality schedule with $\Delta_m = -1.9485$, early peak reproduction, with $\Delta_f = -12.2130$ ($\circ$), age-independent reproduction ($\square$), and delayed peak reproduction, with $\Delta_f = 3.1922$ ($\triangle$), $\Delta_f = 9.9659$ ($+$), $\Delta_f = 15.1978$ ($\diamond$), and $\Delta_f = 20.5213$ (∇) (b).

The first term before taking the expected value can be re-written as

$$\begin{aligned}\ln\{1+\tilde{\delta}\left(\frac{b^*}{\tilde{\delta}}e^X-1\right)\} &= \ln\{1+\tilde{\delta}(e^{\mu+X}-1)\}\\ &= \ln\left\{1+\tilde{\delta}\left(\mu+X+\frac{1}{2}(\mu+X)^2\right)\right\}+o((\mu+X)^2)\\ &= \tilde{\delta}\left(\mu+X+\frac{1}{2}(\mu+X)^2\right)-\frac{1}{2}(\tilde{\delta})^2(\mu+X)^2\\ &+\ o((\mu+X)^2). \qquad (42)\end{aligned}$$

Taking expected values of Eq. (42) by noting that

$$E(\mu+X)^2=\mu^2+EX^2=\mu^2+\sigma^2=\sigma^2+o(\sigma^2),$$

we obtain

$$\tilde{\delta}\mu+\tfrac{1}{2}\tilde{\delta}(1-\tilde{\delta})\sigma^2.$$

Substituting this into Eq. (41) then yields

$$\bar{r}=\tilde{\delta}\mu+\frac{1}{2}\tilde{\delta}(1-\tilde{\delta})\sigma^2-\frac{b^*\Delta_f^{(1)}-\tilde{\delta}\Delta_m^{(1)}}{1+b^*-\tilde{\delta}}\bar{r}+o(\bar{r}). \qquad (43)$$

Solving Eq. (43) for $\bar{r}$, we get

$$\bar{r}=\frac{\tilde{\delta}\mu+\frac{1}{2}\tilde{\delta}(1-\tilde{\delta})\sigma^2}{1+(b^*\Delta_f^{(1)}-\tilde{\delta}\Delta_m^{(1)})/(1+b^*-\tilde{\delta})}+o(\bar{r}). \qquad (44)$$

Since $b^*=\tilde{\delta}e^{\mu}$, we can express Eq. (44) in terms of $\tilde{\delta}$ and μ by noting that

$$\begin{aligned}\frac{b^*\Delta_f^{(1)}-\tilde{\delta}\Delta_m^{(1)}}{1+b^*-\tilde{\delta}} &= \frac{\tilde{\delta}(e^{\mu}\Delta_f^{(1)}-\Delta_m^{(1)})}{1+\tilde{\delta}(e^{\mu}-1)}\\ &= \frac{\tilde{\delta}(\Delta_f^{(1)}-\Delta_m^{(1)}+\mu\Delta_f^{(1)})}{1+\tilde{\delta}\mu}+o(\sigma^2)\\ &= \tilde{\delta}(\Delta_f^{(1)}-\Delta_m^{(1)}+\mu\Delta_f^{(1)})(1-\tilde{\delta}\mu)+o(\sigma^2). \qquad (45)\end{aligned}$$

Substituting Eq. (45) back to Eq. (44) now gives

$$\begin{aligned}\bar{r} &= \frac{\tilde{\delta}\mu+\frac{1}{2}\tilde{\delta}(1-\tilde{\delta})\sigma^2}{1+\tilde{\delta}(\Delta_f^{(1)}-\Delta_m^{(1)}+\mu\Delta_f^{(1)})(1-\tilde{\delta}\mu)}+o(\sigma^2)\\ &= \frac{\tilde{\delta}\mu+\frac{1}{2}\tilde{\delta}(1-\tilde{\delta})\sigma^2}{1+\tilde{\delta}(\Delta_f^{(1)}-\Delta_m^{(1)})}+o(\sigma^2). \qquad (46)\end{aligned}$$

In Eq. (46), we can see how age-structured mortality and fecundity affect population growth rate. A negative $\Delta_f^{(1)}$ (early peak reproduction), and a positive $\Delta_m^{(1)}$ (type I mortality), increase the absolute value of the population growth rate. For long-lived organisms (small $\tilde{\delta}$), age structure becomes less important, unless mortality and fecundity schedules are of extreme type (i.e., very large $\Delta_m^{(1)}$ and $\Delta_f^{(1)}$), since the denominator of Eq. (46) is close to one. Therefore, in studies of very long-lived organisms, negligence of age-structure, or lumping age classes with similar k_x and δ_x, may be justified.

When mortality and fecundity are uniform across age classes, Eq. (46) reduces to

$$\bar{r}=\tilde{\delta}(\mu+\tfrac{1}{2}\sigma^2(1-\tilde{\delta}))+o(\sigma^2). \qquad (47)$$

An equation very similar to this one, but without the age structured effects, appears in the lottery competition model for the growth of a low-density species in competition with another species (Chesson, 1994). This is not surprising as similar assumptions about stochastic variation appear in both formulations. In a companion article (Dewi and Chesson, 2003), we use the results here to obtain coexistence conditions for the lottery model with age structure.

The accuracy of this approximation to $\bar{r}$ is assessed in Fig. 12. Only the case with structured mortality is considered here because structured fecundity is not expected to produce a different pattern. Fig. 12 shows the plot of $\Delta_m^{(1)}$ against the long-term population growth rate, with σ^2 equals 0.25. Eq. (46) can approximate the population growth rate when $E|[\ln\tilde{b}]|<2.9$. Otherwise, the equation can only capture qualitatively the effect of

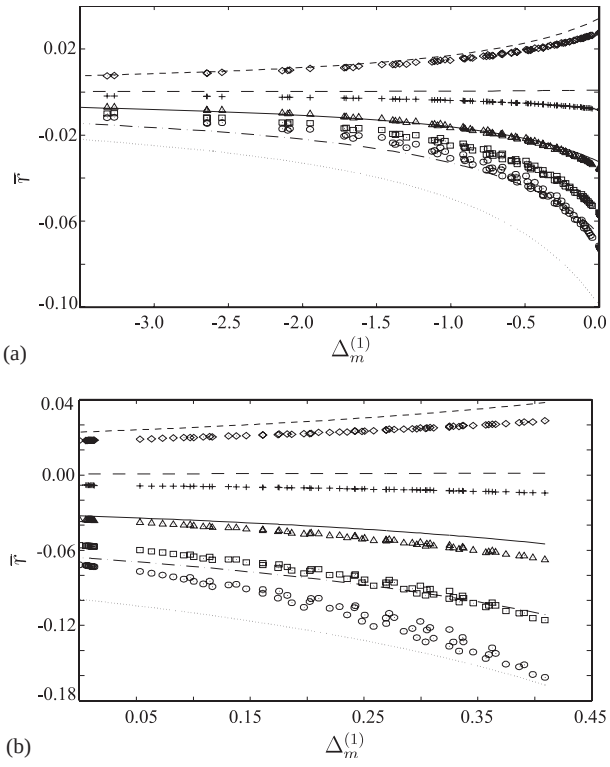

Fig. 12. Population growth rate ($\bar{r}$) with mortality schedules of type I (a), and type III (b), with expected lifetime $= 9$, age-independent reproduction, and $\sigma^2 = 0.25$, calculated from simulation (symbols), and order approximation of Eq. (46) (lines). $E[\ln(\tilde{b})]$ equals -3.2 ($\circ$, dots), -2.9 ($\square$, dots and dashes), -2.6 ($\triangle$, solid), -2.3 ($+$, dashes), and -2 ($\diamond$, short dashes).

different mortality schedules on the population growth rate.

7. Discussion

The proposed shape measures, our Δ-measures, characterize all aspects of the age dependence of mortality and fecundity schedules relevant to determining the population growth rate at stable age structure because then they define the population birth rates and death rates ($\hat{\beta}$ and $\hat{\delta}$) via power series. Our focus above has been primarily on using the first Δ measure in each case to assess the effects of age structure on population growth, but given the fact that these measures characterize the relevant aspects of the shapes of the vital-rate schedules, they suggest a research program to determine more precisely the information provided by these measures. This work in this article is just a beginning. We have used the Δ-measures to obtain approximations to r incorporating structured fecundity and mortality, and these approximations are accurate for small r. More accurate approximations to r would be available by keeping higher than linear terms in the Taylor expansions above. These would necessarily involve Δ-measures beyond first order, and therefore would allow the investigation of more subtle features of age structure on population growth than can be represented by the first-order Δ-measures that have been our focus.

Our results based on the Δ-measures agree with previous findings on the effects of age structure on population growth. In particular, they show that in an increasing population a type I mortality schedule and early peak reproduction have the effect of increasing population growth. On the other hand, in a decreasing population, type III mortality schedules and delayed peak reproduction both reduce the rate of population decline. The approximations to r based on the Δ-measures show that the effects of structured mortality and fecundity schedules should be small for populations of long-lived organisms, subject to the constraint that r is small. This prediction is valid both for deterministically growing and stochastically growing populations. Therefore, for long-lived organisms, negligence of age structure may be justified.

The Δ-measures have application to the study of life-history evolution with the advantage that they summarize age dependence for the entirety of a vital-rate schedule. Thus, their application stands in contrast to approaches based on sensitivity analysis in which the effects of single vital rate are revealed. A previous approach due to Caswell, called macroparameter analysis (Caswell, 1982), is in essence a numerical sensitivity analysis of λ with respect to summary life-history parameters associated with structured mortality and fecundity, e.g., reproductive lifespan, mean age at reproduction, and net reproductive rate. Caswell concluded that a type III mortality schedule, longer lifespan, delayed reproduction, and iteroparity were all favored when populations decline, with the opposite results when populations increase. Our study supports these conclusions and shows a more detailed and general pattern. Caswell used the parameters of parametric curves to summarize the characteristics of vital-rate schedules. Our Δ-measures yield a nonparametric approach to the same ends, and are therefore capable of achieving greater generality.

Acknowledgments

We are grateful for comments on an earlier version of this from Stephen Ellner, Hugh Possingham, and an anonymous reviewer. Support was provided in part by an AusAid Scholarship to Sonya Dewi and NSF grant DEB-0129833 to Peter Chesson.

References

Bernadelli, H., 1941. Population waves. J. Burma Res. Soc. 31, 1–18.

Caswell, H., 1978. A general formula for the sensitivity of population growth rate to changes in life history parameters. Theor. Popul. Biol. 14, 215–230.

Caswell, H., 1982. Life history theory and the equilibrium status of populations. Am. Nat. 120 (3), 317–339.

Caswell, H., 2001. Matrix Population Models: Construction, Analysis, and Interpretation. Sinauer Associates, Inc. Publishers, Sunderland, MA.

Charlesworth, B., 1994. Evolution in Age-structured Populations. Cambridge University Press, Cambridge.

Chesson, P., 1994. Multispecies competition in variable environments. Theor. Popul. Biol. 45 (3), 227–276.

Chesson, P., Ellner, S., 1989. Invasibility and stochastic boundedness in monotonic competition models. J. Math. Biol. 27, 117–138.

Cohen, J.E., 1977. Ergodicity of age-structure in populations with Markovian vital rates. II. General states. Adv. Appl. Prob. 9, 18–37.

Dewi, S., 1998. Structured models of ecological communities in fluctuating environments. Ph.D. Thesis, The Australian National University.

Dewi, S., Chesson, P., 2003. The age-structured lottery model. Theor. Popul. Biol. 64, 331–343.

Ellner, S., 1989. Convergence to stationary distributions in two-species stochastic competition models. J. Math. Biol. 27, 451–462.

Gradshtein, I.S., Ryzhik, I.M., 1980. Table of Integrals, Series, and Products. Academic Press, London.

Kozlowski, J., 1993. Measuring fitness in life-history studies. TREE 8 (3), 84–85.

Law, R., Morton, R.D., 1996. Permanence and the assembly of ecological communities. Ecology 77, 762–775.

Leslie, P.H., 1945. On the use of matrices in certain population mathematics. Biometrika 33, 183–212.

Leslie, P.H., 1948. Some further notes on the use of matrices in population mathematics. Biometrika 35, 213–245.

Lopez, A., 1961. Problems in Stable Population Theory. Princeton University Press, Princeton, NJ.

Oli, M.K., Dobson, F.S., 2003. The relative importance of life-history variables to population growth rate in mammals: Cole's prediction revisited. Am. Nat. 161 (60), 422–440.

Roff, D.A., 1992. The Evolution of Life Histories. Chapman and Hall, London.

Stearns, S.C., 1992. The Evolution of Life Histories. Oxford University Press, New York.

Tuljapurkar, S.D., 1982. Population dynamics in variable environments. III. Evolutionary dynamics of r-selection. Theor. Popul. Biol. 21, 141–165.

Tuljapurkar, S., 1990. Population dynamics in variable environments. In: Lecture Notes in Biomathematics, Vol. 85. Springer, Berlin, Heidelberg.

Tuljapurkar, S., 1997. Stochastic matrix models. In: Tuljapurkar, S., Caswell, H. (Eds.), Structured-population Models in Marine, Terrestrial, and Freshwater Systems. Chapman & Hall, London, pp. 59–88.